PREDICTING BRIDGE BEARING DEMANDS THROUGH A PROBABILISTIC FRAMEWORK

PREDICTING BRIDGE BEARING DEMANDS THROUGH A PROBABILISTIC FRAMEWORK

By

BRYANNA M. NOADE, B.Sc.E. (Civil Engineering)

A thesis Submitted to the School of Graduate Studies in Partial Fulfilment of the Requirements for the Degree Master of Applied Science

McMaster University

Master of Applied Science (2018)
(Civil Engineering)

McMaster University
Hamilton, Ontario

Title:	Predicting Bridge Bearing Demands Through a Probabilistic Framework
Author:	Bryanna M. Noade
Supervisor:	Dr. Tracy C. Becker
Number of Pages:	x, 42

ABSTRACT

The life expectancy of bridge bearings is not well understood or predicted, and bearing replacement is primarily determined through field inspection and engineering judgement. An improved estimate of the timeline for bearing replacement would aid in maintenance scheduling and budgets. As a first step in determining the age for replacement, the annual and lifetime cyclic demands must be estimated. The bearing displacements are largely caused by temperature fluctuation, seismic events, and traffic cycles. In this dissertation a probabilistic framework is presented to quantify the annual cyclic displacement demands on a bearing from these diverse loadings using an archetype continuous concrete girder bridge. The likelihood of occurrence per annum of cycles of increasing amplitudes are presented. In addition, the mean and cycle periods which are related to the loading scenario and cycle amplitude are discussed, and a suggested loading protocol is presented. Three locations across Canada are considered, Quebec City, Toronto and Vancouver, to investigate the influence of location on the bearing demands. The annual expected demands can be used for future work on fatigue testing of bearings to better relate to replacement schedule projections for bridge bearings.

ACKNOWLEDGEMENTS

Firstly, I would like to thank my supervisor, Dr. Becker, for her guidance along the way, interest for my well being, and the support one needs to overcome all the hills and valleys that we like to call research. Also, thank you to Dr. Wiebe for putting Dr. Becker and myself in contact at the start of this all.

The completion of my degree would not have been possible without my friends and department colleagues. Thank you to Kevin McNamara and Alex Sciascetti who brainstormed with me during the tough times and brought laughter to every conversation. My biggest appreciation goes to Paul Steneker, who encouraged me through the low points and celebrated with me during the highs of this degree. I can honestly say that his excitement for my research sometimes exceeded my own.

I would like to thank the owners and chefs at The Mule, the best taco restaurant in Hamilton, ON. Without their consistent offering of the brussels sprout taco over the last two years, I might not have made it through this journey.

Finally, I want to thank my parents for encouraging me to pursue my interests, even as it has taken me away from home. Also, I would not have accomplished what I have today if it were not for my two older brothers and my best friend, Courtney Rent, for providing me with such a steep competition while growing up.

For all of you who, on top of hearing the complaints, witnessed tears along the way, thank you for always encouraging me to move forward. This journey started

with an email and ends with two years of memories and an unquantifiable amount of skills and knowledge. I'll raise a taco to that!

TABLE OF CONTENTS

LIST OF TABLES

LIST OF FIGURES

1 INTRODUCTION

Bridge bearings support the bridge deck, transferring the bridge loads to the substructure, while allowing translation and rotation of the deck under temperature fluctuations and traffic loading. Deteriorated bearing performance can lead to potential damage of surrounding structural components, when movement is restricted it results in a build up of stresses within the structure. This was the case in 2008 for the Birmingham Bridge in Pennsylvania where seized bearings caused damage to the approach structure with an estimated repair cost of $8 million (Grata 2008). Bearing manufacturers and bridge owners have little information regarding at what age the performance of the bearing is compromised. The commentary of the Canadian Highway Bridge Design Code (CHBDC) (CSA 2014b) and AASHTO LRFD Bridge Design Specification (AASHTO 2012) state that bearings must be replaceable due to lack of knowledge of bearing longevity. Thus, bridge bearings are expected to be replaced at some point within a bridge's 50 to 75 year lifespan, depending on which version of the bridge code was used at the time of design. As this is the only guidance, the decision on bearing replacement is left to engineering judgement based on visual field inspections.

There is limited research investigating the life expectancy of bridge bearings. Kumar et al. (2008) found that the probability of bridge failure increases as the structure ages due to the accumulation of damage from small repeated loadings. This suggests that capturing the lifetime loading is more critical than quantifying

extreme events when predicting failure or life expectancy. Roeder et al. (1990) performed experimental fatigue tests on steel-reinforced elastomeric bearings which found that the fatigue behaviour is influenced by loading type, rate, and magnitude. However, the experimental loading procedure used by Roeder et al. was not representative of actual variable-amplitude cyclic loading patterns experienced by a bearing over its lifetime. Ala et al. (2016) performed research on the life expectancy of sliding bridge bearings, focusing on the wear rate (mm/mile) of the sliding surface material. In the study, the total distance travelled by a bearing was predicted from traffic loading and temperature fluctuations to estimate the service life of the wearing surface. Many codes, such as the CHBDC (CSA 2014a), AASHTO (2012), and Ontario Provincial Standard Specification (OPSS) (2016), outline bearing testing and acceptance criteria; however, they are primarily tailored towards approval of the bearing materials. Bearing tests include static holds at maximum displacement/load cases to address the bearing's capacity in extreme weather and traffic. This is not representative of lifetime loads, which are critical when assessing life expectancy.

The primary objective of this study is to quantify the cyclic annual bearing demands derived from multiple load types. In the research presented above (Roeder et al. 1990 or Ala et al. 2016) loading types were investigated independently and the variation in cycle amplitudes or means were not investigated. Furthermore, research on seismic performance of bridge bearings have been investigated separately from

traffic and temperature fatigue loading (i.e. Konstantinidis et al. 2008, Steelman et al. 2013, 2016).

In this study, a framework for calculating the probabilistic bridge bearing demands is outlined, combining the cyclic loading from temperature fluctuation, earthquake events, and traffic loads. Due to the lack of recorded in field bearing demands, in this study, the displacement loading time history is established for various loading scenarios. Rainflow counting is then performed in the time domain to quantify the attributes of the displacement cycles: mean, amplitude, number of occurrence, and duration. Using this, a proposed loading protocol is presented for use in future study on bearing life expectancy. The bearing demands and loading history can be used by bridge owners or researchers to investigate bearing deterioration and set performance goals for bearings.

For the purpose of presenting the framework in its entirety, an example bridge is used and assumptions are made where available data is lacking. However, the framework and loading history presented in this study can be adapted for various bridge designs, bearing designs, locations, and loading types, and can result in a various measures of bearing demands including appropriate fatigue loading protocols or total distance travelled.

2 METHODOLOGY

The bridge bearing demands from temperature, earthquake, and traffic events are first analyzed separately before being combined. The bearing loading varies with geographical region. For this study an archetype bridge designed for a location near Quebec City is used and redesigned for two other Canadian cities, Toronto and Vancouver.

2.1 ARCHETYPE BRIDGE

The archetype bridge is modelled after the Chemin des Dalles Bridge over Highway 55, located in Trois-Rivières, Quebec, Canada. The bridge dimensions, material properties, and dynamic properties are given by Tavares et al. (2013) and Roy et al. (2010). While it is important to realistically model the bridge structure to accurately quantify the bearing demands, the details used here are only to implement the framework.

The bridge, shown in Figure 1, has three 35.5 m spans, supported by two concrete bents and two abutments. A single bent, shown in Figure 2, has three 0.914 m diameter columns joined at their tops by a 1.25 m square beam support. The bridge deck is concrete and supported by six equally spaced AASHTO-type V precast concrete girders. The total mass of the superstructure is roughly 1.6×10^6 kg. The pier drift under lateral seismic loads calculated according to the CHBDC (CSA 2014a) is kept constant for the three cities in this study. The bearing connections

Figure 1: Chemin des Dalles Bridge (Tavares et al. 2013 and Roy et al. 2010)

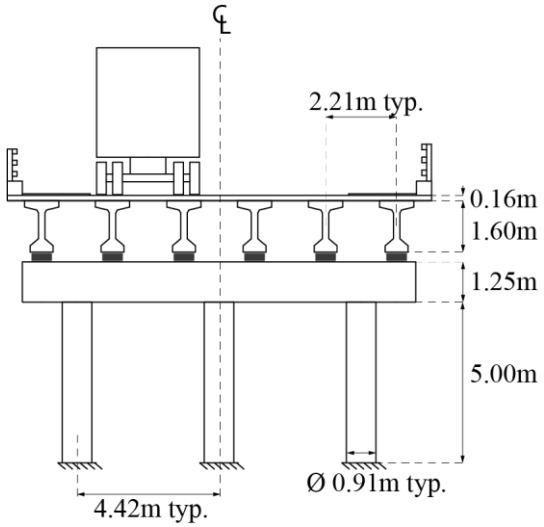

Figure 2: Cross-section of Chemin des Dalles bridge

between the superstructure and bents allow for rotations of the deck but are fixed in the translational degrees of freedom, while steel-reinforced elastomeric bearings are used at the abutments to allow for translation. There are six bearings at each support location, one per concrete girder.

The elastomeric bearings are designed to reach a maximum shear deformation of 50% the total rubber thickness under code temperature loading. The design

displacement is calculated based on the effective construction temperature, also known as set temperature, and the maximum and minimum effective temperatures given in the CHBDC (CSA 2014a) adjusted for concrete material and a girder depth of 1.6 metres. For example, Quebec City's minimum and maximum effective temperatures are -27.5°C and 33.8°C, respectively. The set temperature for the bearings, at which they have zero displacement, is assumed as 15°C. The longitudinal design displacement for the expansion bearings at the abutments, based on the 42.5°C change, the span length, and the thermal coefficient of the material, is 22.6 mm for Quebec City. Using the same process, the design displacement is 21.6 mm for Toronto, and 14.1 mm for Vancouver. The horizontal and vertical stiffness values of the bearing are governed by the design displacement and the maximum compressive axial load on the bearing. The bearing's specifications are given in Table 1. The allowable compressive deflection is calculated as a percentage of the total rubber thickness and is provided by the manufacturer; for example, Goodco (2010) gives the maximum allowable vertical displacement as $0.07T_{eff}$, seven percent of the total rubber thickness between the laminates. This deflection is used as the vertical design displacement in this study,

Table 1: Expansion bearing properties

Location	Width (mm)	Length (mm)	Thickness (mm)	Horizontal Stiffness k_{eff} (kN/mm)	Vertical Stiffness k_v (kN/mm)	Horizontal Design Disp. (mm)	Vertical Design Disp. (mm)
Quebec City	400	300	75	2.39	301.7	22.6	4.2
Toronto	400	300	70	2.63	392.2	21.6	3.9
Vancouver	400	300	60	3.28	380.3	14.1	3.4

with values of 4.2 mm for Quebec City, 3.9 mm for Toronto, and 3.4 mm Vancouver.

The bridge is modelled in OpenSees (McKenna et al. 2010), shown in Figure 3, to assess the bearing demands from regional seismic activity. The superstructure and bents are modeled with elastic-beam column elements with 2% damping. The bridge bearings are modelled with zero length elements with equivalent longitudinal and transverse material properties. To match the in-situ measured periods (Roy et al. 2010) a bilinear model for the rubber bearings with very low yield strength was used (Figure 3). This resulted in an effective stiffness at the design displacement of 2.39 kN/mm for Quebec City, 2.63 kN/mm for Toronto, and 3.28 kN/mm for Vancouver. The resulting first-mode period is 0.38 and 0.64 seconds in the transverse direction for Quebec City and Toronto, respectively, and 0.31 seconds in the vertical direction for Vancouver.

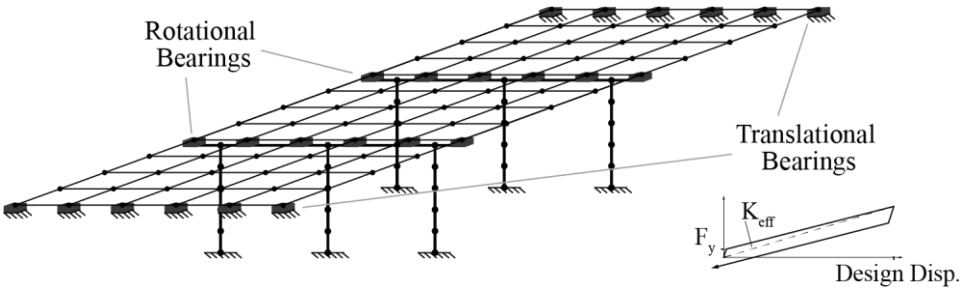

Figure 3: OpenSees bridge model

2.2 TEMPERATURE

The thermal gradients within a bridge deck (Rojas 2014, Krkoska and Moravcik 2017) lead to non-uniform expansion and contraction of the deck resulting in bending and bearing rotations. However, here it is assumed that the entire length, depth and width of the deck reaches the ambient temperature. Historical records of daily maximum and minimum temperatures are available from Environment Canada (2017). A year of temperature data is converted to a time history of thermal expansions and contractions of the bridge deck using the thermal coefficient of concrete, $10x10^{-6}$m/(mK), which is then used to find the displacements of the bridge bearings. Figure 4 shows temperature data and the corresponding bearing displacement for the first week of January and July in the same year. Using the rainflow cycle counting method (ASTM 1997, FEMA 2007), commonly used in fatigue analysis, the number of cycles and their respective mean and amplitude are measured from the temperature displacement history. Table 2 lists the rainflow cycle counts which correspond to the bearing displacement trends in Figure 4.

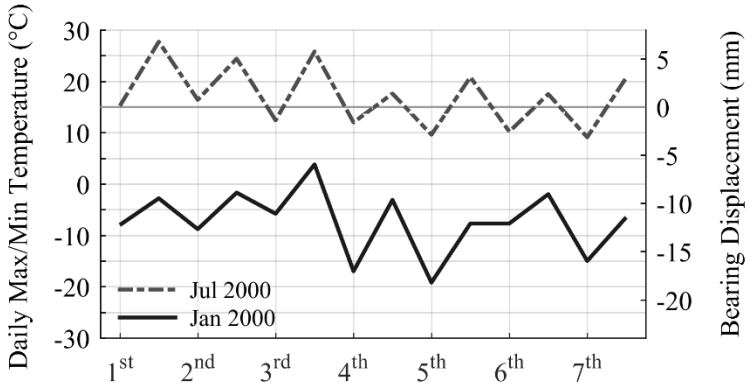

Figure 4: Temperature trends and corresponding bearing displacements for a one-week period in Quebec City

Table 2: Rainflow cycles from data in Figure 4

JANUARY 1st - 7th, 2000			JULY 1st - 7th, 2000		
Cycle Amp. (mm)	Cycle Mean (mm)	Cycle Count	Cycle Amp. (mm)	Cycle Mean (mm)	Cycle Count
1.4	-10.9	0.5	2.5	2.6	0.5
1.6	-11.1	0.5	2.1	2.9	1
1.1	-10.0	1	3.3	3.4	0.5
3.4	-9.3	0.5	3.6	2.2	1
3.7	-13.3	1	1.5	-0.1	1
6.1	-12.1	0.5	1.9	-0.6	1
4.6	-13.6	0.5	3.0	0.1	1
3.5	-12.5	0.5	5.0	1.8	0.5
2.3	-13.7	0.5	-	-	-

For this study, 50 consecutive years of temperature data is used to accurately capture temperature trends as suggested by Guay and Bouaanani (2016). Using the cycle counts for all 50 years of data, a joint annual probability density of the cycle amplitudes (A) and cycle counts (N) is created, shown in Figure 5. From here, the conditional probability of a cycle count given an amplitude, $P_{N \mid A}(n \mid a)$, is derived

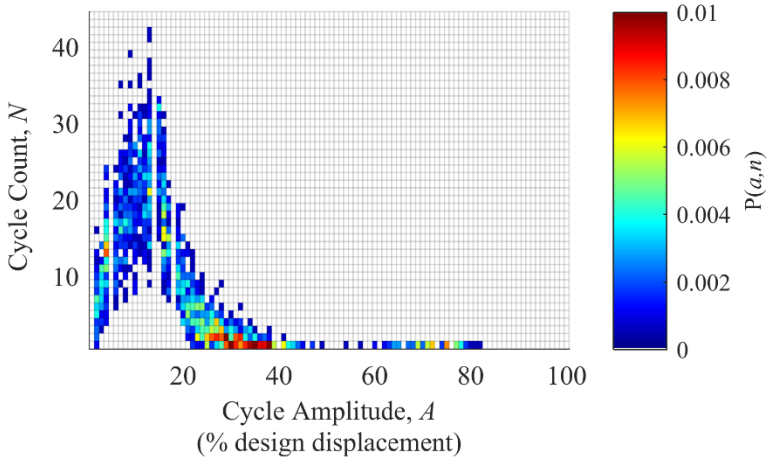

Figure 5: Annual joint probability density from Quebec City temperature data

by dividing the corresponding joint probability, $P_{A,N}(a,n)$, by the marginal probability of cycle amplitude, $P_A\,(a)$, shown in Figure 6. The expected cycle count in a year can then be found for a single amplitude as

$$[1]\; E_{N\mid A}(n\mid a) \;=\; \sum_{all\; n}\; n * \; P_{N\mid A}(n\mid a)$$

For this analysis the amplitudes are binned in intervals of 1-15%, 15-30%, 30-50%, 50-80%, 80-120%, and 120-160% bearing design displacement. Cycles with amplitudes less than 1% design displacement are excluded from this study. The mean annual number of cycles for an amplitude bin results from the summation of the expected cycle count over all amplitudes within the bin.

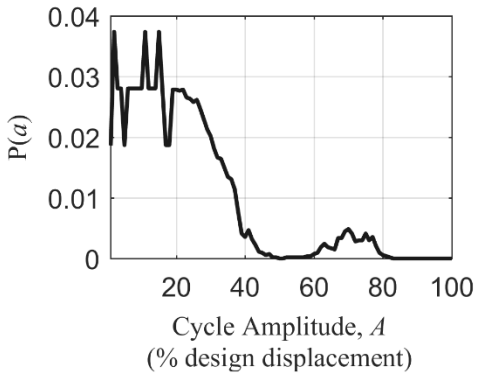

Figure 6: Marginal probability of random variable amplitude from Quebec City temperature data

2.3 EARTHQUAKE

To evaluate the bearing displacement cycles from earthquake loading, a range of earthquake intensities with varying probability of occurrence should be considered. For this study, ground motion suites scaled to design spectras for 2%, 10%, and 40% probability of exceedance in 50 years (mean annual rates of exceedance, λ, of

0.000404, 0.0021, 0.01) are used. The bridges for the three Canadian cities are assumed to be on site Class C, very dense soil or soft rock. The selection and scaling methods presented in the CHBDC and Tremblay et al. (2015) are used in conjunction with the site specific deaggregation values given in Table 3. The spectral acceleration values for the target response spectrum, S(T), are modified from the procedure in the CHBDC for periods less than 0.5 seconds, as shown in Figure 7. The plateau at short periods, used in the CHBDC, does not reflect actual spectral acceleration demands for periods below 0.5 seconds. While this is conservative and useful for equivalent static methods, it leads to an unrealistic target spectrum for ground motion matching. A more accurate calculation of the short period spectral accelerations is presented in Tremblay (2015).

Ground motions are scaled from 0.2 times the first mode period to 1.5 seconds as outlined in the commentary for the CHBDC (2014b). For Quebec City and Toronto synthetic ground motions suites for Eastern North America from Atkinson (2009)

Table 3: Mean deaggregation values for a period of 0.3 seconds (Canadian Hazards Information Service, 2017)

	Probability of Exceedance in 50 years	Mean Distance (km)	Mean Magnitude (Mw)
Quebec City	2%	34	6.48
	10%	66	6.34
	40%	123	6.25
Toronto	2%	67	6.3
	10%	150	6.28
	40%	269	6.2
Vancouver	2%	66	7.17
	10%	74	7.09
	40%	80	6.8

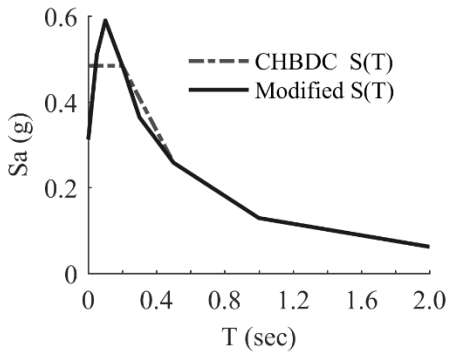

Figure 7: Quebec target response spectrum for 2%/50 years

are selected and scaled for the three probability of exceedances. The synthetic ground motion files have 15 three-component sets of ground motions. The resulting ground motion response spectra are shown in Figure 8. For both Quebec City and Toronto, at lower periods, the average response spectrum of the scaled motions is much larger than the target response spectrum. This is because the average response spectrum of the scaled ground motions must be greater than 90% the target response spectrum within the period range for scaling; thus, the longer period range of the target spectrum controls the scaling. For Vancouver, for both 40% and 10% probability of exceedance in 50 years the suite of ground motions is comprised of recorded strike slip records from the PEER Strong Motion Database (Chiou 2008). For 2% probability of exceedance in 50 years, three subduction records are included using lightly-modified real recordings from the Tokachi Oki earthquake from Atkinson and Macias (2009). For this return period, the strike slip records are scaled within the lower period range, less than 0.75 seconds, while the subduction records are scaled to larger periods, shown in Figure 8.

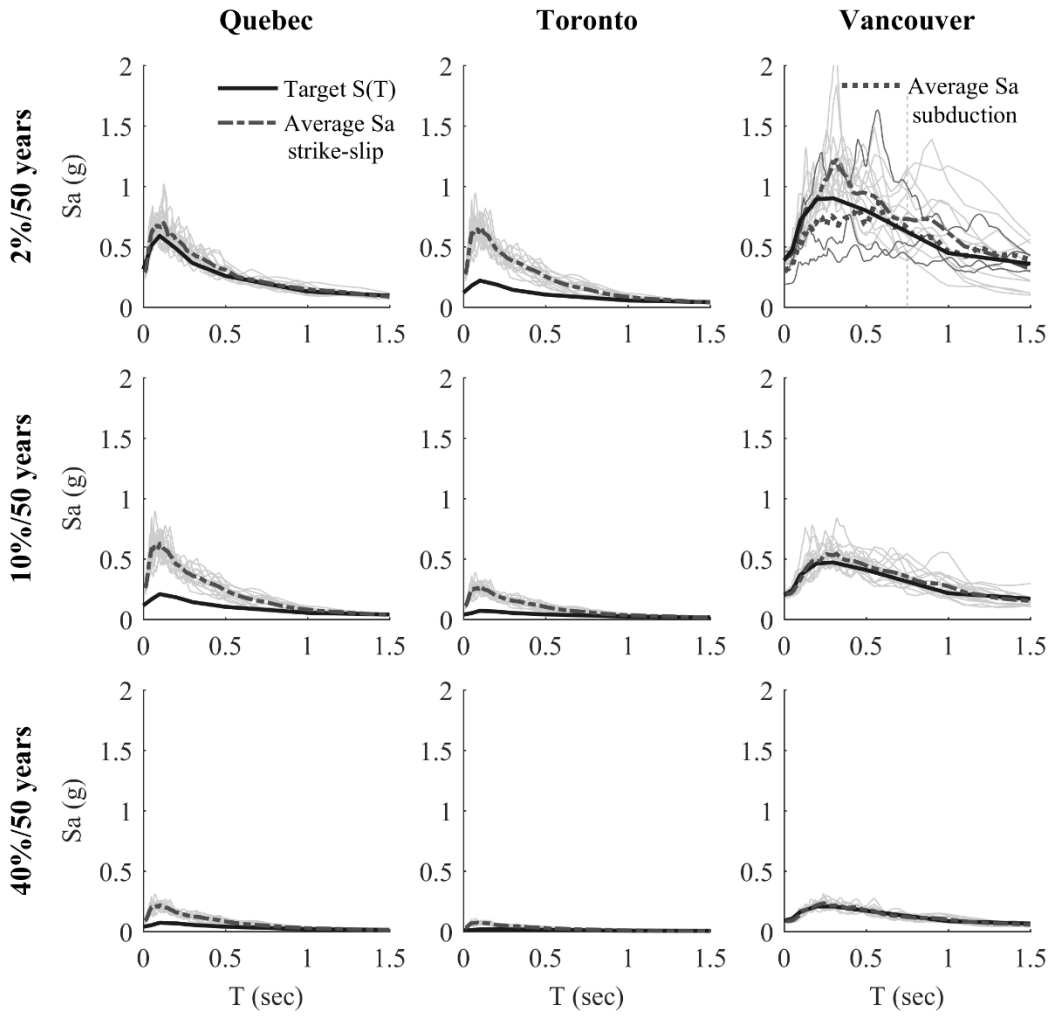

Figure 8: Scaled response spectra

The OpenSees model of the archetype bridge is then subjected to the ground motion suites. The bearing displacement history is recorded for each ground motion, and rainflow counting is again used to extract the number of cycles of varying amplitudes from which joint probability densities are created for each hazard level. Because nonseismic bridge bearings are used, which have a small level of damping, the amplitude range of 0-1% design displacement has significantly larger cycle counts than other ranges. As these are very small motions, they are ignored.

Examples of the joint probabilities for the three hazard levels, $P_{A,N \mid \Lambda}(a, n \mid \lambda)$, are shown in Figure 9. Each joint probability is divided by the corresponding marginal probability of the cycle amplitude to achieve the conditional probability for each hazard level, $P_{N \mid A,\Lambda}(n \mid a, \lambda)$. Following this, the cyclic demands for the three hazard levels are combined to achieve the probability of exceedance in a single year through

[2] $P_{N \mid A}(n \mid a) = \sum_{all\ \Delta\lambda} P_{N \mid A,\Lambda}(n \mid a, \lambda) * \Delta\lambda$

where $\Delta\lambda$ is the range of annual rate of exceedance that each hazard level represents found from the hazard curve as shown in Figure 10. The expected cycle count for a given amplitude a is then calculated using Equation 1 and then summed for each amplitude over the bin.

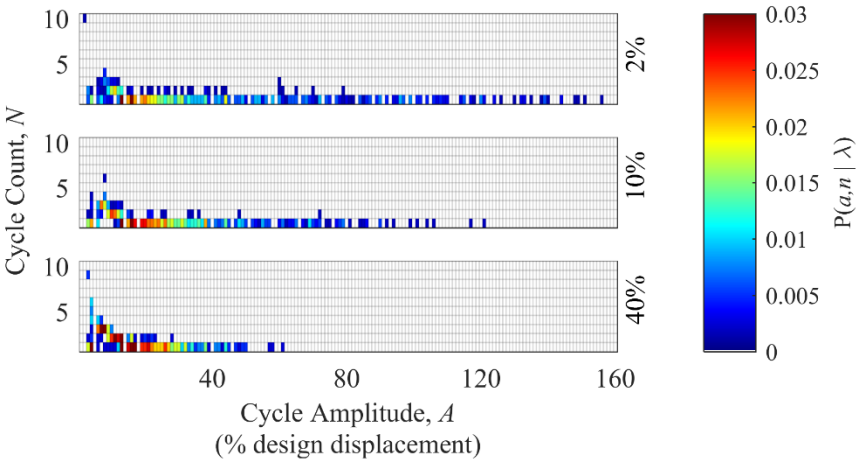

Figure 9: Joint probability densities for the longitudinal direction from Quebec City seismic data

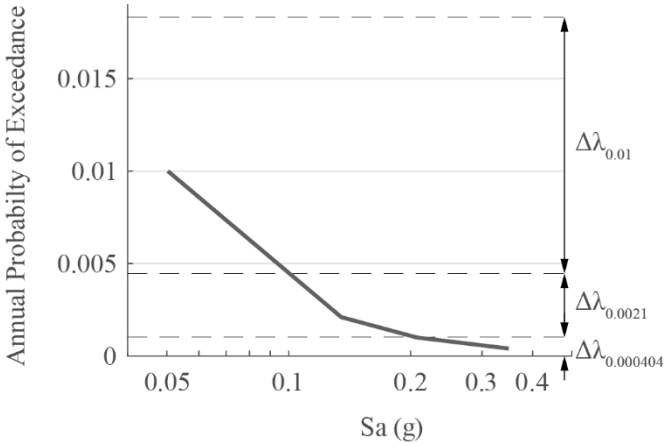

Figure 10: Quebec hazard curve for a period of 0.38 seconds

2.4 TRAFFIC

Typical traffic loading causes cyclic axial loading on the bearings, and longitudinal deformations as a result of vertical deck deflections. Demands caused by braking and acceleration are not considered here. According to the U.S. Government Accountability Office (1979) a single multi-unit truck causes the equivalent damage to 9,600 passenger vehicles on the road. Thus, only multi-unit trucks, the heaviest vehicle category on highways with a gross vehicle weight rating of greater than 14,971 kg, are considered. In this study a CL-625 truck (CSA 2014a) is used. An S-Frame model of the bridge is utilized to quantify the axial and longitudinal displacements as a result of the moving load. Unlike temperature or seismicity, the traffic loading is assumed to be the same for the three Canadian cities. The displacement history of the translational abutment bearings varies slightly depending on which abutment is observed, as shown in Figure 11, because of the

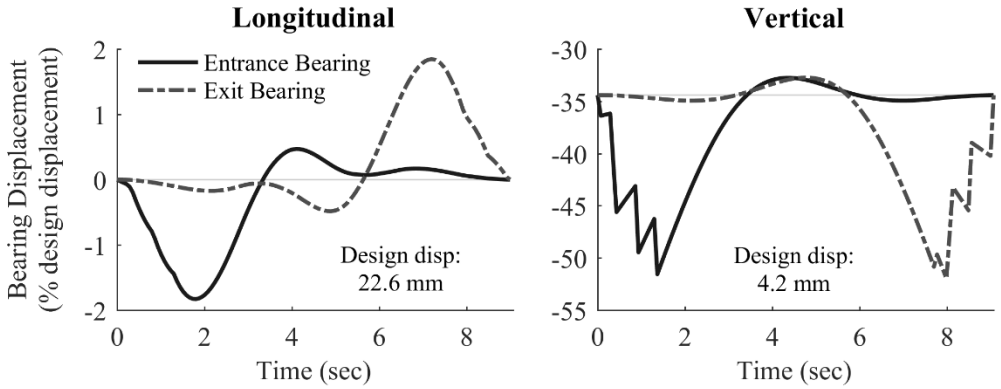

Figure 11: Traffic loading histories for Quebec City

nonuniform truck axle loads. In this study, the bearings over which the truck enters the bridge on will be analyzed.

To capture the longitudinal deformation of the expansion bearings due to traffic, a moving load of the CL-625 truck is applied to the S-Frame model. The longitudinal displacement of the bearings, caused by bending of the deck under the loading, is shown in Figure 11. The maximum longitudinal displacement of the abutment bearings is 0.4 mm for all three locations. The rate at which the truck drives across the bridge is assumed to be the posted highway speed limit, 50 km/h, resulting in a nine second passing over the bridge. Using the rainflow cycle counting method thenumber of cycles and their respective mean and amplitude are measured from the displacement history, shown in Figure 11.

The Chemin des Dalles Bridge carries two lanes of traffic, one in either direction, with a shoulder on both sides, and is supported on six bearings at each support location (see Figure 2). Due to the symmetric layout of the bearings and lanes, a conservative assumption is made that the axial wheel loads for a lane of traffic act

in line with two girders, and thus are only transferred to the two bearings directly below. Applying a moving load of a CL-625 truck across the two-girder S-Frame model results in a maximum axial bearing load of roughly 220 kN. The bearing's vertical stiffness can then be used to find the vertical displacement demand, shown in Figure 11.

The vertical displacement is centered about the static gravity load displacement in the range of -1.0 to -1.5 mm for all three locations. The maximum vertical displacement caused by a multi-unit truck (CL-625 truck) is -2.2 mm for Quebec City, and -1.7 mm both for Toronto and Vancouver. From the displacement history shown in Figure 11, the rainflow cycle counting method can be used to measure the number of cycles and their respective mean and amplitude.

To evaluate the traffic load's expected cycle counts per annum, the traffic flow rate q is quantified using the average vehicle speed profile for one of Canada's busiest highways, Highway 401 in Ontario (Ferguson et al. 2016). Although Highway 401 is not representative of the traffic over the Chemin des Dalles Bridge, due to the lack of available traffic data this speed profile is used to calculate annual traffic counts and the values are later reduced with an assumption on vehicles exiting the highway at this single controlled access. The user of this framework should use the most accurate traffic data available for the bridge under analysis. The profile is used to find the average density in passenger car units (pcu) per mile per lane at each time of day (Canadian Capacity Guide 2008), shown in Table 4. The flow rate, q,

in terms of pcu per hour per lane, is calculated by multiplying the average speed by the corresponding average density.

The Canadian Capacity Guide (2008) outlines the passenger car unit equivalents (pcu/vehicle) for different vehicle categories; for example, multi-unit trucks pcu/veh equals 2.5. On the 401 highway, multi-unit trucks comprise 3% of the vehicles while single unit trucks cover 21%, and passenger cars 76% (Ministry of Transportation of Ontario 2006). Combining the flow rate, and the percentage of vehicles and passenger car unit equivalent for each vehicle category, the number of vehicles per hour in a single lane can be quantified as

[3] $(veh/hr/ln) = q/(\sum [\,\%\, of\ veh * (pcu/veh)\,])$

Multiplying the vehicles per hour per lane by 3% results in the multi-unit trucks per hour per lane and is calculated for each separate time period. With the assumption that each directional lane on the bridge is loaded equally with multi-unit trucks, total cycle counts in a day can be determined, as given in Table 4. This can be extended to a per annum basis like the temperature and seismic analysis. Since the Chemin des Dalles Bridge is an overpass for a controlled highway access it is assumed 5% of the multi-unit trucks per day, calculated for Highway 401, is representative of the truck traffic on the bridge.

Table 4: Estimated daily schedule based on speed profile and corresponding vehicle rates

Time Period	Average Speed (km/hr)	Average Density (pcu/mi/ln)	Vehicle Rate (veh/hr/ln)	Multi-unit Truck Rate (m.u.t/hr/ln)	Multi-unit Truck Count (m.u.t/ln)
0:00 – 6:59	115	5.5	344	10	72
7:00 – 9:59	70	40.5	1550	46	139
10:00 – 14:59	90	22.5	1096	33	164
15:00 – 19:59	60	40.5	1303	39	195
20:00 – 23:59	115	5.5	344	10	41

3 BEARING DEMANDS

3.1 ANNUAL EXPECTED CYCLE COUNTS

The expected cycle counts, which are essential for developing fatigue loading histories, give the expected number of cycles per annum for each value of amplitude defined by intervals of one percent design displacement. Amplitudes less than one percent design displacement have been excluded in this study. Note that the bearing design displacements are different between the three locations; the horizontal and vertical design displacements for Quebec City are 22.6 mm and 4.2 mm, for Toronto are 21.6 mm and 3.9 mm, and for Vancouver are 14.1 mm and 3.4 mm, respectively. It is the specific city's design displacement that is referenced when presenting cycle amplitude in percentage of design displacement.

3.1.1 Temperature

The expected cycle counts from the longitudinal thermal expansion and contraction of the bridge deck caused by temperature fluctuations are presented in Figure 12. Bearing rotations and transverse translations are not considered here. For the three locations evaluated in this study, Quebec City, Toronto, and Vancouver, the shape of the expected number of cycles versus amplitude values is consistent between regions. The maximum cycle counts observed occur between amplitudes of 5-20% design displacement and range up to 23 to 25 cycle counts per annum. All three regions experience maximum cycle amplitudes between the range of 80-90%

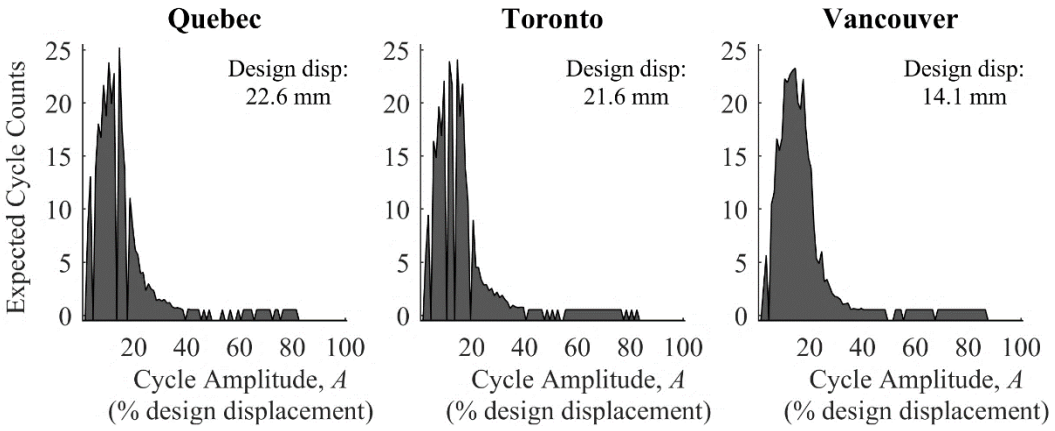

Figure 12: Temperature annual expected cycle counts longitudinally

design displacement. While each region has different temperature demands, as the bearing design is dependent on the design displacement, the cyclic demands are similar across Canada which is useful from a fatigue testing protocol perspective.

3.1.2 Earthquake

The expected cycle counts from the bearing displacement during seismic events are presented in Figure 13 for all three cities. The cycles were analyzed for the bearing's three translational degrees of freedom, longitudinal, transverse, and vertical. Because the seismic events have a low probability per annum, 0.000404, 0.0021, and 0.01 for the three return periods included in this study, the expected cycle counts are typically below 0.1 cycles.

The cycle amplitudes for both horizontal directions are measured in terms of the horizontal design displacement. For each location, the longitudinal and transverse directions have similar expected cycle counts, this is especially true for Vancouver. For Quebec City, the expected cycle counts in the longitudinal direction are larger than for

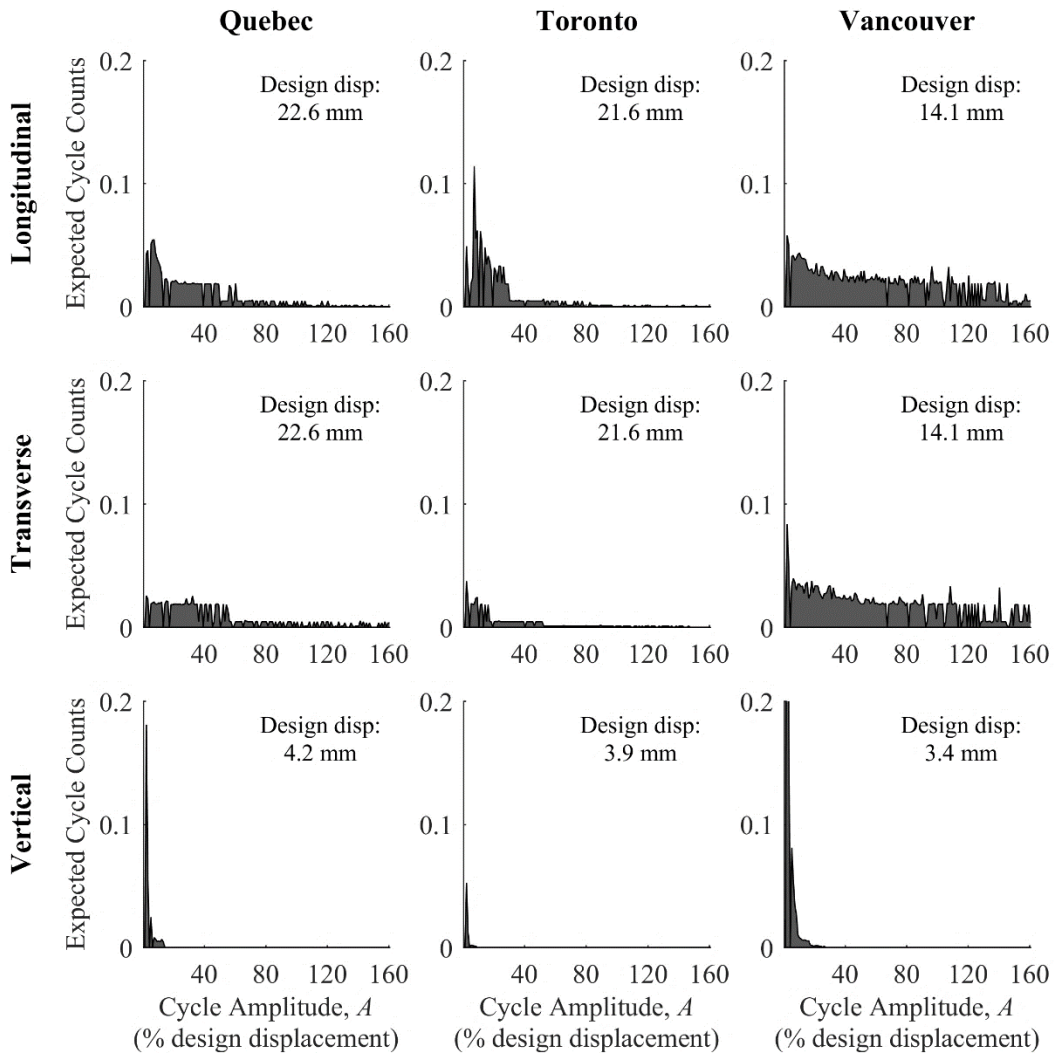

Figure 13: Seismic annual expected cycle counts

the transverse direction in the amplitude range of 0-15% design displacement and smaller in the 120-160% design displacement range. This difference is because the first dynamic mode of the bridge is in the transverse direction; thus, larger displacement cycles are expected transversely. A similar trend can be seen for Toronto, which also has a transverse first mode, although the total expected cycle counts are less than Quebec. The expected cycles in the two horizontal directions for Vancouver have very

similar trends, because for this design, the first longitudinal and transverse dynamic modes of the bridge have similar periods.

The cycle amplitudes for the vertical direction are measured in terms of vertical design displacement, which is significantly smaller than the horizontal design displacement. The cycle amplitudes range up to 15%, 10%, and 30% vertical design displacement for Quebec City, Toronto and Vancouver, respectively. The size of the amplitude range has a positive correlation with the seismicity of the location.

3.1.3 Traffic

The expected cycle counts from the bearing displacement due to traffic loading are presented in Figure 14 for bins of one percent design displacement. Both the

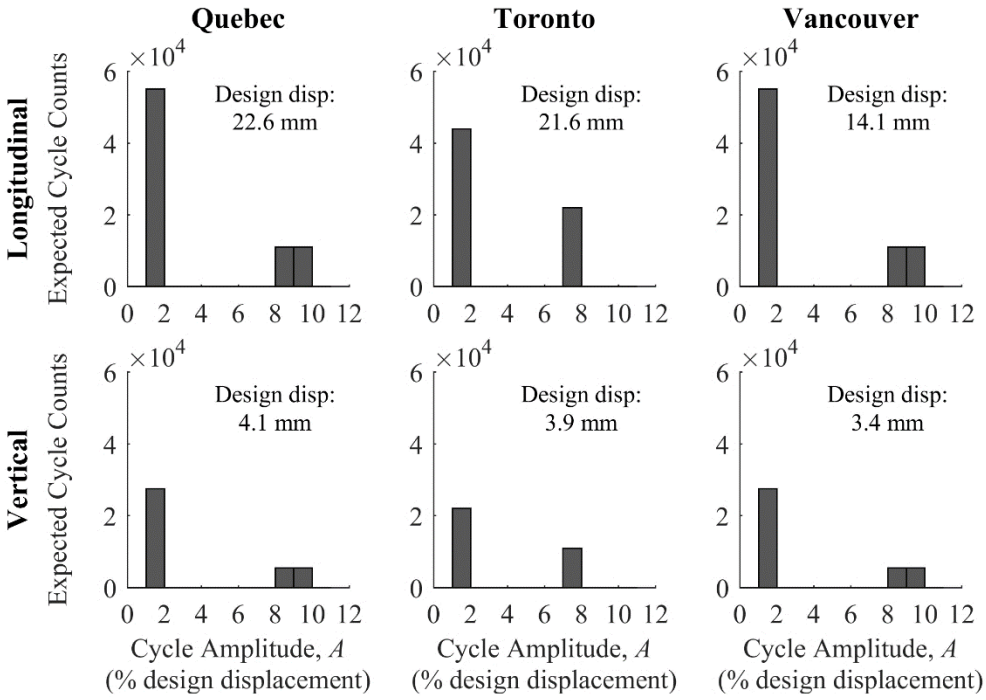

Figure 14: Traffic annual expected cycle counts

longitudinal and vertical displacement histories of the bearings (Figure 11) are comprised of small cycles below an amplitude of 10% design displacement. Using the assumptions described previously, there are roughly 22,000 multi-unit trucks passing over the bridge per year. Although the amplitudes are small, in combination with the large cycle counts, the total longitudinal distance travelled by the bearing due to traffic in a year is over 24 m, thus, a large contributor to life time wear.

3.1.4 Comparison of Demands

The cycle amplitudes are binned in intervals of 1-15%, 15-30%, 30-50%, 50-80%, 80-120%, and 120-160% bearing design displacement. The mean annual number of cycles for an amplitude bin results from the summation of the expected cycle count over all amplitudes within the bin. The mean annual number of cycles are presented for the longitudinal, transverse, and vertical directions respectively in Table 5, Table 6, and Table 7.

For the longitudinal direction, the annual number of expected cycles from temperature fluctuations is significantly greater than those from seismic events for the Canadian cities (Table 5), with the exception of the largest amplitude bin. Although seismic expected cycle counts are small, it is important to capture them because the larger cycle amplitudes, in the 120-160% design displacement range, are not seen from temperature or traffic. Vancouver has larger cycle counts from seismic loading, especially in the larger amplitude bins, because of its higher seismicity. The longitudinal expected cycle counts caused by traffic are hundreds

Table 5: Longitudinal mean annual expected cycle counts per amplitude range

Range of Design Disp.	TEMPERATURE			SEISMIC			TRAFFIC		
	Que.	Tor.	Van.	Que.	Tor.	Van.	Que.	Tor.	Van.
1-15%	225.31	198.46	218.52	0.47	0.54	0.54	77,000	66,000	77,000
15-30%	73.94	90.86	134.70	0.27	0.36	0.42	0	0	0
30-50%	18.12	21.53	21.04	0.31	0.09	0.49	0	0	0
50-80%	20.00	26.00	27.00	0.15	0.08	0.63	0	0	0
80-120%	2.00	2.00	7.00	0.07	0.02	0.64	0	0	0
120-160%	0	0	0	0.01	0.01	0.33	0	0	0

Table 6: Transverse mean annual expected cycle counts per amplitude range

Range of Design Disp.	SEISMIC		
	Que.	Tor.	Van.
1-15%	0.24	0.22	0.51
15-30%	0.27	0.08	0.44
30-50%	0.28	0.08	0.48
50-80%	0.15	0.03	0.58
80-120%	0.09	0.03	0.61
120-160%	0.06	0.02	0.34

Table 7: Vertical mean annual expected cycle counts per amplitude range

Range of Design Disp.	SEISMIC			TRAFFIC		
	Que.	Tor.	Van.	Que.	Tor.	Van.
1-15%	0.30	0.07	1.04	38,500	33,000	38,500
15-30%	0	0	0.02	0	0	0
30-50%	0	0	0	0	0	0
50-80%	0	0	0	0	0	0
80-120%	0	0	0	0	0	0
120-160%	0	0	0	0	0	0

of times larger than those caused by temperature fluctuations. This is explained by the repetitiveness of traffic loading, 61 multi-unit trucks per day, while only one temperature cycle occurs during the same time period.

The only load case considered in the transverse direction is from seismic activity (Table 6), showing a positive correlation between expected cycle counts and the city's seismicity. Toronto sees the least cycles followed by Quebec City and then

Vancouver. A similar trend is seen for both longitudinal and vertical seismic results as well. As the transverse demands from seismic activity are comparable to those in the longitudinal direction, and seismic is the only contributing load in the transverse direction, transverse loading is excluded from the protocol.

In the vertical direction, the expected number of cycles caused by traffic loading is much greater than those from seismic activity. Similar to the longitudinal traffic results in Table 5, traffic loading has a much higher rate of occurrence in comparison to seismic return periods explaining the larger difference between expected counts. Thus, seismic loading does not need to be considered for the vertical demands.

3.2 CYCLE MEANS AND FREQUENCIES

While the number and amplitude of the cycles is important, so is the mean about which the bearing cycles as it controls the peak bearing displacement.

3.2.1 Temperature

Figure 15 depicts the relationship between displacement cycle amplitude, mean, and period from the temperature loading for Quebec City. The average cycle mean is based on an average temperature of 4°C for Quebec City. Thus, the design displacement of the bearings could be reduced if the set temperature of the bearings was closer to 4°C than 15°C. Similarly, for Toronto and Vancouver the average cycle means occur around 8°C and 10°C, respectively, as shown in Figure 16. While there is little to no correlation between cycle amplitude and mean, there is a

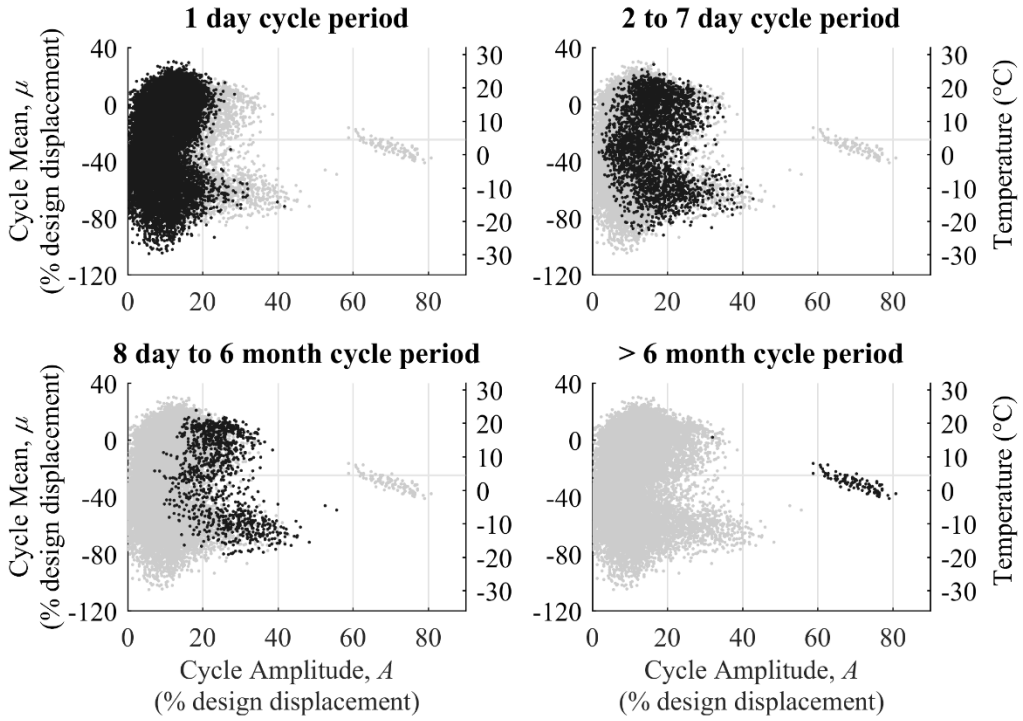

Figure 15: Mean of cycles versus cycle amplitude for Quebec City

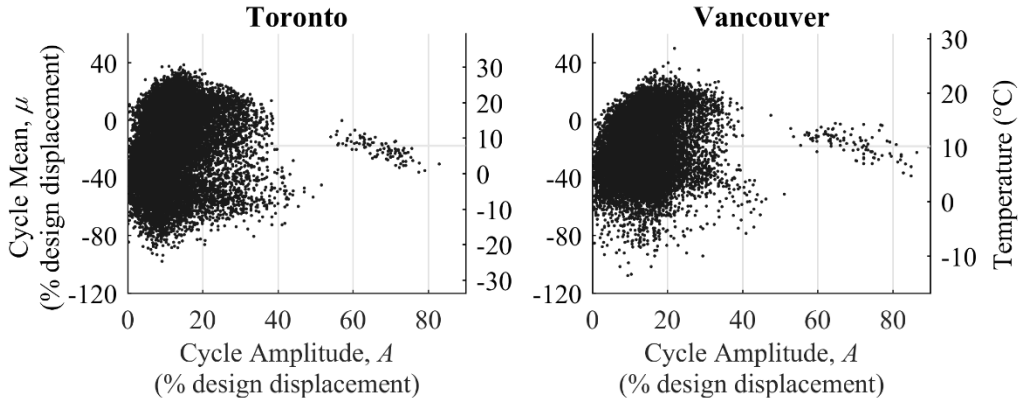

Figure 16: Mean of cycles versus cycle amplitude

positive correlation between the cycle amplitude and the cycle period. Daily temperature fluctuation causes displacement cycles with amplitudes in the range of 0-20% design displacement, where as temperature fluctuations between 8 days and 6 months cause displacements within 20-40% of the design displacement. Much

larger cycle amplitudes (60-80%) are caused by yearly temperature fluctuations from the changing seasons. Generally, increasing cycle period relates to smaller deviation in the mean of the cycles. For daily cycles, the means vary across a temperature range of +/- 30°C from the average cycle mean temperature for Quebec City, +/- 25°C for Toronto, and +/-15°C for Vancouver, as they cycle about the daily average temperature. By contrast, for the seasonal cycles, the means of the cycles are within +/- 5°C for all three cities. Interestingly, the cycles with 8 day to 6 month periods have a bimodal distribution of the cycle means. This can be explained as the cycle trends experienced in the extreme seasons of summer and winter. The bimodal distribution is created because the average temperature of these seasons is either above or below the yearly average. The distribution is seen best for Quebec City in Figure 15, because this city has more defined seasons of hot and cold in comparison to Vancouver whose seasons do not have as extreme changes.

3.2.2 Earthquake and Traffic

In contrast to temperature displacement cycles, bearing cycles from earthquakes and traffic cycles have periods of milliseconds to seconds. The mean of the longitudinal displacement cycles is the instantaneous thermal displacement, as shown in Figure 17. Thus, the initial displacement of the bearing and the mean of each cycle can differ by up to the bearing's design displacement, +/- 22.6 mm, 21.6 mm, or 14.1 mm respectively for Quebec City, Toronto, or Vancouver. The mean of the vertical earthquake displacement cycles is the displacement caused by the

gravity load of the superstructure, a value between -1.0 and -1.5 mm for the three locations.

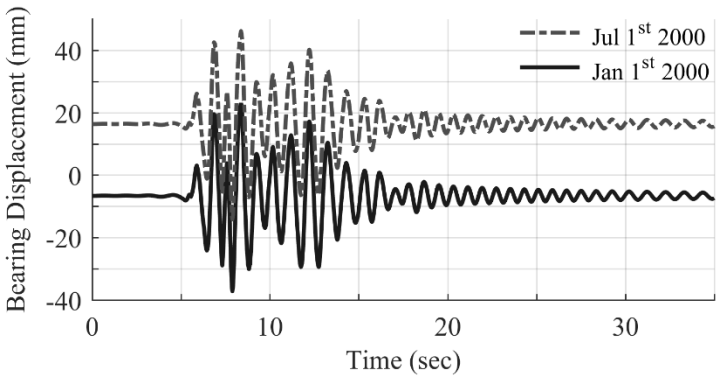

Figure 17: Earthquake displacement history on two different days within the year 2000

4 PROPOSED LOADING HISTORY

Based on the results from the previous sections, the cyclic demands are compiled into a proposed loading history for Quebec City. The loading protocol is location and bridge design specific. The aim is to develop guidance for fatigue loading histories to better evaluate the service life of bridge bearings. Future work is necessary on generalizing the loading.

Damage is a cumulative process that is dependent on the number and relative amplitude of the cycles within a loading history, the sequence of the cycles, the cycle means, and the loading rate. Sequence effects are commonly captured in loading protocols through a conservative assumption that cycle amplitudes increase as the loading history proceeds (FEMA 2007), which is used here. This allows damage to be evaluated over increasing demands and avoids immediate failure of the test specimen. For many seismic loading protocols (ATC-24, SAC, CUREE, FEMA 461, etc.) cycle means and loading rates (cycle periods) are not taken into consideration (Krawinkler 2009). This results in cycles centered about zero and a loading history defined only by cycle number. For the development of this loading history, a constant longitudinal cycle mean is not representative as it does not capture the expected variation in means caused by seasonal temperature changes, as shown in Figure 15 and Figure 16. Due to experimental duration restraints, accurate loading rates are typically not addressed in test procedures; however, they can be important to specific tests, such as when evaluating wear rate as done by Ala

et al. (2016). The fatigue loading history presented here does not include loading rate, but it should be addressed when damage is rate dependent.

The bearing loading history is comprised of four segments with varying cycle means, as shown in Figure 18. This achieves two goals: to capture the mean effects that occur during the summer and winter seasons, and to capture the large amplitude temperature cycles resulting from yearly temperature fluctuations. Two segments (1 and 3) are cycled about the average cycle mean from the long period temperature loading (> 6 month cycle period), -30% design displacement for Quebec City (see Figure 15). Two remaining segments (2 and 4) are cycled at the midpoint between the long period cycle mean (-30%) and the extreme cycle mean values (-106%, 31%), shown in Figure 19. For Quebec City the cycle means of these two segments are -70% and 2% design displacement. The cycle means of the loading history segments are indicated on Figure 19 by vertical dashed lines, note that segment 1 and 3 are represented by the same value. With the addition of smaller cycles within the segments of the loading history (Figure 18) the total displacement range of the

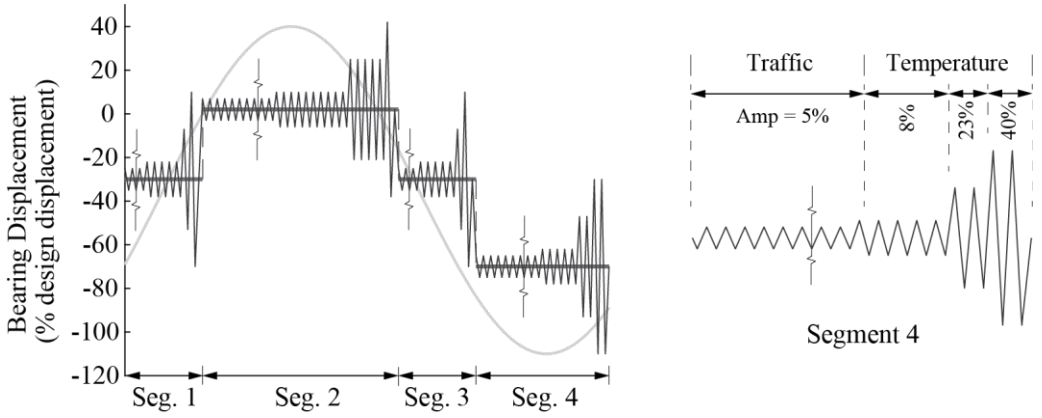

Figure 18: Example fatigue loading history

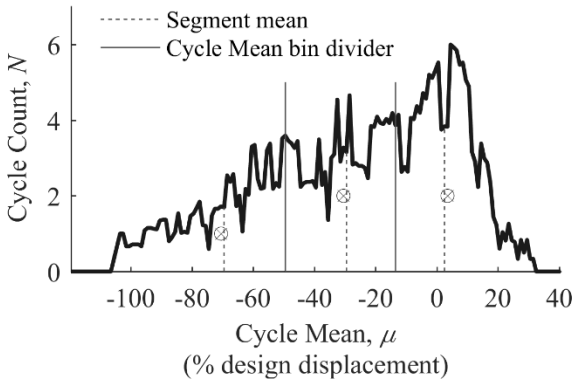

Figure 19: Expected cycle counts versus cycle means for Quebec City temperature data

bearing from peak to peak is roughly 140% design displacement, thereby capturing long period temperature cyclic demands which have an average amplitude of roughly 70% design displacement.

The smaller temperature cycles, from amplitude bins 1-15%, 15-30%, and 30-50% design displacement, along with the traffic expected cycles which are within an amplitude of 1-10% design displacement, are distributed across these four segments. For each amplitude bin, the median is used as the representative cycle amplitude, 8%, 23%, and 40% for temperature and 5% for traffic. To appropriately distribute the cycles between the segments, the expected cycles for each amplitude range are binned by mean, as represented by Figure 19 and shown in Figure 20. The dividers for the three cycle mean bins, shown in Figure 19, are placed so that the centroid of each section (represented with a cross in Figure 19) aligns with the three segment means (-70%, -30%, and 2%), so that half of the cycles in each bin have means that occur above and below the segment mean. For Quebec City the dividers are at cycle mean values of -50% and -14% design displacement. Using the cycle

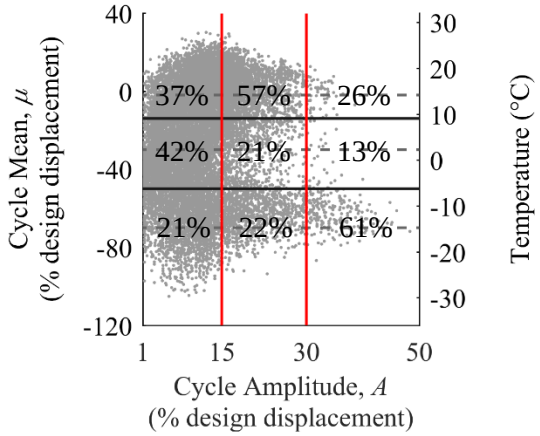

Figure 20: Binned cycle mean versus amplitude for Quebec City temperature data

mean versus amplitude relationship and the bin dividers, shown in Figure 20, the percentage of temperature cycles for each segment of the loading history is determined individually for each amplitude bin (1-15%, 15-30%, 30%-50%). Note that the center cycle mean bin represents both segment 1 and 3 and that the percentage of cycles is divided amongst the two segments equally. Multiplying by the corresponding expected total cycle counts for that amplitude bin, given in Table 5, results in the number of temperature cycles of each amplitude per segment, given in Table 8. The distribution of traffic cycles across the loading history segments is based on the percentage of temperature cycles in each cycle mean bin in Figure 20, which is representative of the duration of each segment over the year.

Table 8: Cycles within each segment of a fatigue loading history for Quebec City

Loading History Segment	TEMP			TRAFFIC	SEISMIC*					
	8%	23%	40%	5%	8%	23%	40%	65%	100%	140%
1	48	8	1	9,625	-	-	-	-	-	-
2	82	42	5	30,800	-	-	-	-	-	-
3	48	8	1	9,625	-	-	-	-	-	-
4	47	16	11	26,950	5	3	3	2	1	0

* applied at the end of every 10th consecutive loading history

As seismic events cause less than one full cycle expected per annum, for simplicity when testing, they can be added once full seismic cycles have been accumulated, for example every ten years for Quebec City. Although seismic events have an equal likelihood of occurrence throughout the year, it is easiest to apply the seismic cycles to the end of the tenth loading history. Adding these cycles to the last segment of the loading history, which represents the winter months, is a conservative approach as it results in the largest total bearing displacement.

Unlike for longitudinal, a complementary vertical fatigue loading history does not have to have varying cycle mean but rather a constant static offset between -1.0 and -1.5 mm. Traffic cycles per annum would be applied at this cycle mean. If test equipment allows, this vertical fatigue loading should be applied in parallel with the longitudinal loading to best replicate real demands.

5 CONCLUSIONS

This paper uses a probabilistic framework to quantify displacement demands on bridge bearings within Canada due to three load cases: temperature fluctuations, seismic events, and traffic loading. Procedures to find the cycle amplitude, mean, and number of occurrence per annum were presented using an example bridge with elastomeric bridge bearings at the abutments. The temperature demands, in terms of bearing design displacement, were found to be identical across the three example cities within Canada. The largest cycle amplitude within a year falls around 80% design displacement caused by the change of seasons, which shorter period temperature demands cycle around. The most common cycle amplitudes from daily temperature changes are between 5% and 20% design displacement. Traffic cycles, although having amplitude values below 10% design displacement, dominate the expected cycle counts in the longitudinal and vertical direction because of their rate of occurrence.

As would be expected, the range of amplitude values and expected cycle counts from earthquakes has a positive correlation with the seismicity of the location. The number of annual expected seismic cycles are significantly smaller but can include larger amplitude cycles that exceed the bearing's horizontal design displacement, unlike temperature and traffic loading whose amplitudes stay below the design displacement. Research is needed to understand the effect of the combination of the

low cycle fatigue caused by temperature and traffic with these extreme seismic cycles on the fatigue and failure of bridge bearings.

The longitudinal displacement demands from multiple loadings were compiled into a fatigue loading history, defined in terms of the bearing's design displacement so it can be easily modified for different bearing designs. While the procedure would be the same, the number, means, and amplitudes of the cycles are dependent on the bridge structure and bearing type. The demand caused by traffic loading accounts for 99% of the cycles and total distance travelled by the bearing within the loading history, however does not contribute to any cycles above 10% of the bearing's displacement capacity.

The framework and loading history presented in this study can be adapted for various bridge designs, bearing designs, locations, and loading types. While previous studies look at purely total distance traveled or demands from individual loading types, this study presents a path towards a loading history that can be used to test the performance of bearings under realistic lifetime loading. The findings highlight diverse loading amplitudes for various loading types as well as a need to test at increased cyclic means to account for yearly temperature changes. Using a more representative fatigue loading history for bearings will allow bearing manufacturers and bridge owners to better quantify the service life of bridge bearings, leading to more accurate forecasting of replacement schedules and costs.

6 RECOMMENDATIONS FOR FUTURE STUDY

6.1 BRIDGE MODEL

The archetype bridge modelled after the Chemin des Dalles Bridge is a simplistic bridge design and a good starting point to establish the methodology presented in this paper. Further research should look into the bearing demands of other common bridge designs within Canada; such as steel-girder, box-girder, truss, or orthotropic deck bridges. Additionally, the bridge bearings are modelled as reinforced elastomeric bearings, further studies should evaluate the change in demands across various bearing designs used in Canada; such as sliding, pot, or lead rubber plug bearings.

6.2 ROTATIONAL DEMANDS

Rotational bearing demands were not accounted for in this study; however, bearings have rotation limits and this loading, by itself or in combination with horizontal and/or vertical displacement demand, could potentially cause deterioration. Similar to the demands presented in the previous sections, the rotational demands caused by the three loadings can be quantified as a percentage of the design rotation. While this would be straightforward for traffic or seismic demands, in this study, a uniform temperature across the depth of the superstructure was used. While this is an appropriate assumption to find the longitudinal displacement demands on the

bridge bearings caused by temperature fluctuations, rotational demands would be underestimated.

6.3 EARTHQUAKE ANALYSIS

The CHBDC (2014a) defines two approaches for scaling earthquake records: linear scaling and spectral matching. In this study, synthetic time histories and recorded ground motions were linearly scaled along the scaling period range defined in the commentary of the CHBDC (2014b). The result of this scaling is that, for both Quebec City and Toronto, at lower periods, the average response spectrum of the scaled motions is much larger than the target response spectrum, see Figure 8. This is because the average response spectrum of the scaled ground motions must be greater than 90% the target response spectrum within the period range for scaling, thus, the longer period range of the target spectrum controls the scaling. A different scaling approach might be considered to achieve a better match over the target spectrum in any further research on this topic.

For this study the three locations were assumed to all have site Class C. Peak seismic demands will vary slightly with site classes. While this may affect the number and amplitudes of the larger cycles. The change in the number of lower cycles will be negligible when combined with temperature and traffic. Thus, the effect of the site class is expected to be small.

6.4 TRAFFIC ANALYSIS

In reality, the traffic demands on a bridge widely vary with location and the category of road. For this study, the traffic demand is assumed constant for all three locations and is quantified using recorded vehicle data from Highway 401 in Ontario, with an assumption of the number of trucks entering/exiting the highway at the overpass. With more accurate knowledge of the traffic demands, the bearing demands can be better estimated. This is especially true as traffic loading dominates the low amplitude cycle demands.

Further research on the displacement demands of bridge bearings from traffic loading should also include braking forces on the deck. Additionally, centrifugal forces would add transverse demands on the bearings on curved bridges. These forces are both addressed in the CHBDC for bridge design but not in this study.

7 REFERENCES

AASHTO. 2012. LRFD Bridge Design Specifications. American Association of State Highway and Transportation Officials, Washington, DC, USA.

Ala, N., Power, E.H., and Azizinamini, A. 2016. Predicting the Service Life of Sliding Surfaces in Bridge Bearings. Journal of Bridge Engineering, 21(2): 04015035

ASTM. 1997. Standard Practices for Cycle Counting in Fatigue Analysis E 1049-85. American Society for Testing Materials, West Conshohocken, PA, USA.

Atkinson, G. M. 2009. Earthquake time histories compatible with the 2005 National building code of Canada uniform hazard spectrum. Canadian Journal of Civil Engineering, 36: 991-1000.

Atkinson, G. M. and Macias, M. 2009. Predicted Ground Motions for Great Interface Earthquakes in the Cascadia Subduction Zone. Bulletin of the Seismological Society of America, 99(3): 1552-1578.

Canadian Hazards Information Service. 2017. Seismic Hazard Deaggregation.

Chiou, B., Darragh, R., Gregor, N., and Silva, W. 2008. NGA Project Strong-Motion Database. Earthquake Spectra: February 2008, Vol. 24, No. 1, pp. 23-44

CSA. 2014a. Canadian Highway Bridge Design Code S6-14. CSA Group, Toronto, ON, Canada.

CSA. 2014b. Commentary on CSA S6-14, Canadian Highway Bridge Design Code. CSA Group, Toronto, ON, Canada.

Environment Canada. 2017. Historical Climate Data. Retrieved from http://climate.weather.gc.ca/

FEMA. 2007. Interim Testing Protocols for FEMA 461, Determining the Seismic Performance Characteristics of Structural and Nonstructural Components. Applied Technology Council, Redwood City, CA, USA.

Ferguson, M., Harrison, C., Pang, J., Higgins, C. and Kanaroglou, P. 2016. Enhancing Transportation Corridors to Support Southern Ontario Innovation Ecosystems. McMaster University Institute for Transportation and Logistics, Hamilton, ON, Canada.

Goodco Z-Tech. 2010. Elastomeric Bearings [Brochure]. Canada: Canam Group Inc.

Grata, J. 2008, July 1. Birmingham Bridge report confirms rocker bearing failure. Pittsburgh Post-Gazette. Retrieved from http://www.post-gazette.com/breaking/2008/07/01/Birmingham-Bridge-report-confirms-rocker-bearing-failure/stories/200807010159

Guay, L.P. and Bouaanani, N. 2016. Assessment of low temperature exposure for design and evaluation of elastomeric bridge bearings and seismic isolators in Canada. Canadian Journal of Civil Engineering, 43: 851-863.

Konstantinidis, D., Kelly, J.M. and Makris, N. 2008. Experimental Investigation on the Seismic Response of Bridge Bearings (Report No. EERC 2008-02). University of California, Berkeley: Earthquake Engineering Research Center.

Krawinkler, H. 2009. Loading Histories for Cyclic Tests in Support of Performance Assessment of Structural Components. Third International Conference on Advances in Experimental Structural Engineering. San Francisco, CA. October 15-16, 2009. International Association for Experimental Structural Engineering.

Krkoska, L. and Moravcik, M. 2017. Monitoring the Temperature Gradient Development of Highway Concrete Bridge. Proceedings of the XXVI R-S-P Seminar on Theoretical Foundation of Civil Engineering. MATEC Web of Conferences, 117.

Kumar, R., Gardoni, P., and Sanchez-Silva, M. 2008. Effect of Cumulative Seismic Damage and Corrosion on the Life-Cycle Cost of Reinforced Concrete Bridges. Earthquake Engineering Structural Dynamics, 39: 887-905.

McKenna, F., Scott, M.H., and Fenves, G.L. 2010. Nonlinear Finite Element Analysis Software Architecture Using Object Composition. Journal of Computing in Civil Engineering, 24(1): 95-107.

Ministry of Transportation of Ontario. 2015. 2006 Commercial Vehicle Survey: traffic volumes at survey stations. [An inventory of traffic volume summarized by vehicle classes]. Retrieved from https://www.ontario.ca.

Ontario Provincial Standards. 2016. Material Specification for Bearings – Elastomeric Plain and Steel Laminated. OPSS.PROV 1202.

Roeder, C.W., Stanton, J.F., and Taylor, A.W. 1990. Fatigue of Steel-Reinforced Elastomeric Bearings. Journal of Structural Engineering, 116(2): 407-426.

Rojas, E. 2014. Uniform Temperature Predictions and Temperature Gradient Effects on I-Girder and Box Girder Concrete Bridges (Masters theses). Retrieved from Utah State University Libraries: All Graduate Theses and Dissertations. 2193.

Roy, N., Paultre, P., and Proulx, J. 2010. Performance-Based Seismic Retrofit of Bridge Bent: Design and Experimental Validation. Canadian Journal of Civil Engineering, 37: 367-379.

Steelman, J.S., Fahnestock, L.A., Filipov, E.T., LaFave, J.M., Hajjar, J.F., and Foutch, D.A. 2013. Shear and Friction Response of Nonseismic Laminated Elastomeric Bridge Bearings Subject to Seismic Demands. Journal of Bridge Engineering, 18(7): 612-613

Steelman, J.S., Fahnestock, L.A., Hajjar, J.F., and LaFave, J.M. 2016. Performance of Nonseismic PTFE Sliding Bearings When Subjected to Seismic Demands. Journal of Bridge Engineering, 21(1): 04015028

Tavares, D.H., Suescun, J.R., Paultre, P., Padgett, J.E. 2013. Seismic Fragility of Highway Bridge in Quebec. Journal of Bridge Engineering, 18(11): 1131-1139.

Tremblay, R., Atkinson, G. M., Bouaanani, N., Daneshvar, P., Leger, P. and Koboevic, S. 2015. Selection and Scaling of Ground Motion Time Histories for Seismic Analysis using NBCC 2015. The 11th Canadian Conference on Earthquake Engineering. Victoria, BC. July 21-24, 2015. Canadian Association for Earthquake Engineering.

U.S. Government Accountability Office. 1979. Excessive Truck Weight: An expensive burden we can no longer support CED-79-94. U.S. General Accounting Office, Washington, DC, USA.